



Research article

Insights into the consequence of (Al–Zn) dual-doping on structural, morphological, and optoelectrical properties of CdO thin films

M Ashikul Haque Naeem^a, Ahmed Sidrat Rahman Ayon^a, Md. Mintu Ali^{a,*},
Md. Ruhul Amin^b, M. Humayan Kabir^a, Md. Abdus Sattar^b, Samia Tabassum^c, Md
Nurul Huda Liton^{c,d}

^a Department of Glass & Ceramic Engineering, Rajshahi University of Engineering & Technology (RUET), Rajshahi, 6204, Bangladesh

^b Department of Materials Science & Engineering, University of Rajshahi, Rajshahi, 6205, Bangladesh

^c Department of Physics, University of Rajshahi, Rajshahi, 6205, Bangladesh

^d Department of Physics, Begum Rokeya University of Rangpur, Rangpur, 5400, Bangladesh

^e Institute of Energy Research and Development, Bangladesh Council of Scientific and Industrial Research, Dhaka, 1205, Bangladesh

ARTICLE INFO

Keywords:

Cadmium oxide thin film
Zinc–Aluminium dual-doping
Spray pyrolysis
Structural properties
Optoelectrical properties

ABSTRACT

The present study explores the structural, morphological, optical, and electrical properties of spray pyrolyzed (Al–Zn) dual-doped CdO thin films. The un-doped and (Al–Zn) dual-doped CdO thin films have been deposited on glass substrate using spray pyrolysis route at 325 °C. The physical properties of the doped samples were analyzed as a function of Zn concentration (2–5 mol%) with constant Al (3 mol%) concentration. XRD analysis confirms the successful incorporation of (Al–Zn) dual-doping into CdO crystal as well as the polycrystalline nature was evident. No phase transitions were apparent from XRD data while revealing the single cubic structure of all the samples. The surface morphology of the samples studied by SEM. It shows the formation of rock-shaped microstructure and the variation of grain size with doping concentrations. Optical analysis was done using UV–vis spectroscopy within the range of 300–1200 nm. Maximum value of transmittance was attained for 3% (Zn–Al)-doped CdO sample. The dual doping exhibits the broadening of band gap values (2.61–3.84 eV) whereas a decrease in extinction coefficient was noticed as a function of Zn doping concentration. Electrical analysis was done using the four-probe method and a high resistivity was seen for higher Zn concentration. Obtained results and precise comparison with some similar films suggested that 2% Zn and 3% Al co-doping can be a suitable candidate for optoelectronic devices.

1. Introduction

In recent decades, extensive research has been dedicated to semiconductor thin films, particularly in the context of advancing thin-film devices crucial to the field of optoelectronics. A significant class of materials in this domain is Transparent Conductive Oxides (TCOs), possessing the dual attributes of transparency and electrical conductivity. TCOs find widespread application, notably in thin-

* Corresponding author.

E-mail address: mintu@gce.ruet.ac.bd (Md.M. Ali).

<https://doi.org/10.1016/j.heliyon.2024.e26545>

Received 23 December 2023; Received in revised form 14 February 2024; Accepted 15 February 2024

Available online 16 February 2024

2405-8440/Â© 2024 The Authors. Published by Elsevier Ltd. This is an open access article under the CC BY-NC-ND license (<http://creativecommons.org/licenses/by-nc-nd/4.0/>).

film solar cells, flat-panel displays (LCDs and OLEDs), touchscreens, and various electronic devices [1]. The evolution of TCO materials has been marked by the development of binary compounds like SnO_2 and In_2O_3 , followed by the introduction of ternary compounds such as Cd_2SnO_4 , CdSnO_3 , and CdIn_2O_4 [2,3]. The pursuit of enhanced performance has led to the exploration of various thin-film TCO materials, with binary compounds offering advantages in chemical composition control during film depositions compared to more complex ternary and multicomponent oxides [1].

Among these materials, Cadmium Oxide (CdO) stands out for its high transparency, excellent electrical conductivity, and resilience to harsh environments and elevated temperatures, rendering it desirable for specific optoelectronic and electronic applications. Furthermore, CdO contributes to the durability of devices, ensuring their long-term functionality. To fully unlock the potential of CdO thin films in diverse applications such as flat panel displays, solar cells, gas sensors, and smart windows, researchers aim to enhance key properties such as electrical conductivity, optical transmittance, and charge carrier mobility. One promising avenue involves the incorporation of suitable dopants into the CdO lattice to tailor its properties for specific application requirements.

In the field of optoelectronic thin films, doping has emerged as a powerful strategy to tailor the properties of various materials. For instance, doping can alter the properties of ZnO films by combining the transparency of the host material with the electrical properties of carbon nanotubes [4]. Additionally, titanium doping has been shown to significantly impact the optoelectronic properties of ZnO, leading to promising applications in photo detectivity [5]. Furthermore, the addition of semiconductor material TiO_2 has been proven to increase the gas sensitivity of carbon nanotubes [6]. Recent observations indicate that doping CdO with metallic ions having an ionic radius smaller than that of Cd^{2+} improves both electrical conductivity and optical band gap [7]. Additionally, co-doping CdO with other elements, such as Ni and Ga [8], Cu and Fe [9], Eu and H [10], Cu and Mn [11], Zn and Co [12], and Ni and Al [13] was also seen to manipulate the optical and electrical properties.

Among the potential dopants, aluminum (Al) and zinc (Zn) emerge as particularly promising due to their ionic radii, slightly smaller than that of Cd^{2+} . This characteristic facilitates the ready substitution of Zn^{2+} and Al^{3+} ions into the CdO crystal lattice, suggesting potential enhancement of the electrical and optical properties of the CdO crystalline structure through co-doping. Notably, existing research by Azzaoui et al. [14] focused on Al–Zn co-doped CdO thin films, fixing a 3% Zn concentration while varying the Al content. However, the consequences of fixing Al doping concentration while varying Zn concentrations remain unexplored.

Previous studies emphasize the positive impact of Al doping on transparency and conductivity, as well as the reduction of reflectivity [15]. Furthermore, optimal combinations of minimum resistivity, maximum carrier concentration, and maximum transmittance were observed with 3 mol% Al doping in CdO [16]. Usharani et al. [17] demonstrated that increasing Zn concentration in CdO improves both electrical and optical properties, including altering the band gap.

Motivated by these findings, our research aims to investigate (Al–Zn) dual-doped CdO thin films, keeping 3 mol% Al as a fixed concentration while varying Zn content from 2% to 5% maintaining structural homogeneity of the base film. The choice of the spray pyrolysis method for film fabrication stems from its cost-effectiveness, versatility, and precise control over film thickness and doping concentrations. This method is particularly suitable for large-scale industrial implementation. The novelty of our research resides in the fabrication of a double-doped CdO film, with a fixed concentration of aluminum and varying zinc concentration, employing the cost-effective technique of spray pyrolysis while ensuring structural homogeneity of the film. We anticipate that our results will be conducive to enhancing the overall performance of optoelectronic devices. Moreover, these findings have the potential to expand the horizons of fabricating other doped metal oxide thin films, thereby enriching the landscape of optoelectronic materials and their applications. Therefore, after fabricating the thin films by the spray pyrolysis method, we analyze and compare the structural, morphological, optical, and electrical properties of the (Zn–Al) dual-doped CdO thin films to ensure their potential applications.

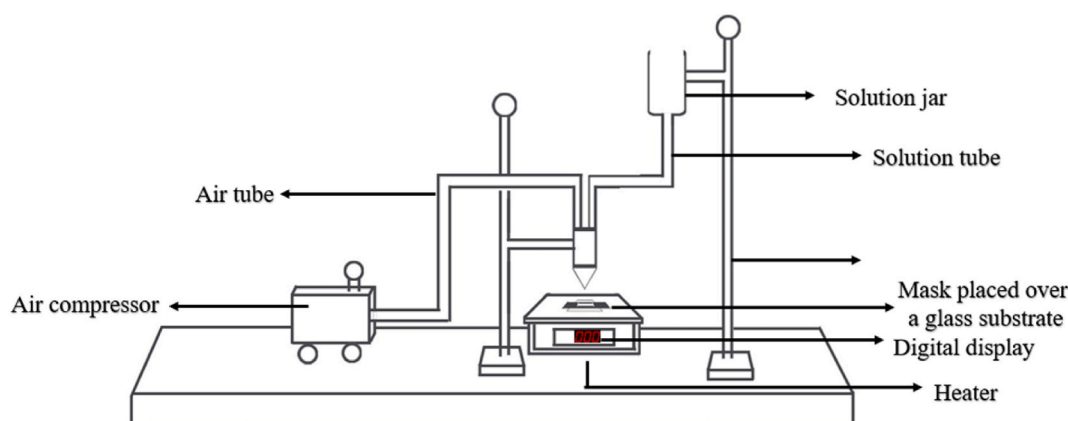
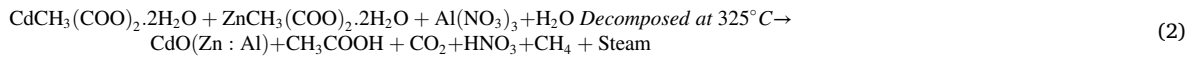


Fig. 1. Schematic diagram of our experimental setup.

2. Materials and methods

2.1. Deposition of thin film

The chemicals used for the deposition included Cadmium acetate dihydrate ($[\text{Cd CH}_3(\text{COO})_2] \cdot 2\text{H}_2\text{O}$) for CdO, aluminum nitrate nonahydrate ($\text{Al}(\text{NO}_3)_3$) for Al, and zinc acetate dihydrate ($[\text{Zn CH}_3(\text{COO})_2] \cdot 2\text{H}_2\text{O}$) for Zn. All chemicals were sourced from Merck KGaA with purity levels of 99%, 98%, and 98.5%, respectively. Glass slides served as substrates, and distilled water was used as the solvent. The preparation of the solution involved dissolving 0.1 M solutions of each material separately prepared in distilled water. The thin films were deposited using the spray pyrolysis method, and the experimental setup is depicted in Fig. 1. The solution was mixed using a magnetic stirrer. The composition of the sprayed solution is detailed in Table 1, with a fixed 3% Al concentration and varying Zn percentages (2%–5%). The solution was atomized through a nozzle, and a heating plate served as the heat source, maintaining a temperature of 325 °C. Prior to deposition, glass substrates were meticulously cleaned with deionized water and organic solvent, followed by drying under normal atmospheric conditions. To prevent thermal shock, the glass substrates were gradually preheated before being placed on the heating plate. For each sample, an air compressor pressure of 1 bar and a liquid flow rate of 1 ml/min were utilized. The solutions were deposited from a vertical distance of 18 cm. This methodology ensured the controlled deposition of undoped and (Al–Zn) dual-doped CdO thin films on glass substrates, providing a basis for subsequent analysis and characterization. The most probable reactions that took place during the deposition process are as follows equations (1) and (2) [15].



After the deposition process, the thin films were thoroughly analyzed and characterized to assess their properties and potential applications.

2.2. Characterization and film analysis

The Bruker X-ray diffractometer (model: D8 Advanced) has been used to study the structural characteristics of CdO and Al–Zn double doped thin films. $\text{CuK}\alpha$ ($K = 1.5406 \text{ \AA}$) X-ray radiation was utilized to examine every sample between 20 and 80 diffraction angles at 25 °C. The average crystallite sizes of CdO and AZCO were determined using the Debye-Scherrer equation (3) [18].

$$D = \frac{K\lambda}{\beta \cos \theta} \quad (3)$$

where D is the crystallite size, λ is the X-ray wavelength (1.5406 \AA), β is the full width at half maximum (FWHM) of the peak (111), θ is the Bragg angle and K depends on the crystallite shape and the size distribution, indices of the diffraction line, and the actual definition used for β whether FWHM or integral breadth [14]. Here we have used a K value of 0.94 representing an estimation of our obtained D value.

To determine the lattice constant parameter a , cell volume V , strain ε , and dislocation density δ , the peak intensity related to the (111) plane has been used. The values of a , V , ε , and δ were calculated using relations (4)–(7) [19].

$$d = \frac{a}{\sqrt{(h^2 + k^2 + l^2)}} \quad (4)$$

$$V = a^3 \quad (5)$$

$$\varepsilon = \frac{\beta \cos \theta}{4} \quad (6)$$

Table 1
Sprayed solution composition.

Sample	Solution composition
CdO	100% $[\text{Cd CH}_3(\text{COO})_2] \cdot 2\text{H}_2\text{O}$ solution
AZCO-1	2% $[\text{Zn CH}_3(\text{COO})_2] \cdot 2\text{H}_2\text{O}$ solution + 3% $\text{Al}(\text{NO}_3)_3$ solution + 95% $[\text{Cd CH}_3(\text{COO})_2] \cdot 2\text{H}_2\text{O}$ solution
AZCO-2	3% $[\text{Zn CH}_3(\text{COO})_2] \cdot 2\text{H}_2\text{O}$ solution + 3% $\text{Al}(\text{NO}_3)_3$ solution + 94% $[\text{Cd CH}_3(\text{COO})_2] \cdot 2\text{H}_2\text{O}$ solution
AZCO-3	4% $[\text{Zn CH}_3(\text{COO})_2] \cdot 2\text{H}_2\text{O}$ solution + 3% $\text{Al}(\text{NO}_3)_3$ solution + 93% $[\text{Cd CH}_3(\text{COO})_2] \cdot 2\text{H}_2\text{O}$ solution
AZCO-4	5% $[\text{Zn CH}_3(\text{COO})_2] \cdot 2\text{H}_2\text{O}$ solution + 3% $\text{Al}(\text{NO}_3)_3$ solution + 92% $[\text{Cd CH}_3(\text{COO})_2] \cdot 2\text{H}_2\text{O}$ solution

$$\delta = \frac{1}{D^2} \quad (7)$$

EVO-18 research scanning electron microscope (Carl Zeiss, UK) was used to characterize the surface morphology of the films. Elemental information is obtained from Energy-dispersive X-ray spectroscopy (EDS) machine (JCM 6000Plus).

The optical transmittance (T), and absorbance (A) of undoped and Al–Zn dual-doped CdO films were investigated using a UV–visible double-beam spectrophotometer (UV-2600) operating in the wavelength range of 300–1200 nm at room temperature.

The following equation (8) well-known Tauc law is used to calculate the optical bandgap of the samples. where α is the absorption coefficient, A is a constant, h is the plank's constant, ν is the frequency of light, E_g is the optical band gap and n is a constant [13].

$$ah\nu = A(h\nu - E_g)^n \quad (8)$$

The absorption coefficient values were measured by using the following equation (9) where T is the transmittance and d is the film thickness [20].

$$\alpha = \frac{\ln \frac{1}{T}}{d} \quad (9)$$

By using the following equations (10) and (11), extinction coefficient(k) and refractive index(n_r) have been measured, where, λ is the wavelength of light and r is the reflectance

$$k = \frac{\alpha\lambda}{4\pi} \quad (10)$$

$$n_r = \frac{1+r}{1-r} \sqrt{\frac{4r}{(1-r)^2 - k^2}} \quad (11)$$

Electrical characterization was done using the four probes van der Pauw method. Silver wire was used as a contact(probe) material. Probes were placed at a distance of 8 mm from each other and the size of the probe was 0.7 mm². At the mid position of the sample, probes were placed. Then, the conductivity and resistivity are measured using equation (12) [21].

$$V = IR \quad (12)$$

Where, I is the current and R is the resistance.

3. Results and discussion

3.1. Structural analysis

Fig. 2 shows the spectra of X-ray diffraction obtained for pure and dual-doped CdO thin films and also the peak shift of the (111) plane. The XRD spectra of pure and dual-doped CdO samples visualized the multiple peaks at crystal faces (111), (200), (220), (311), and (222) which indicates the polycrystalline nature of the films. The XRD spectra suggested the cubic structure for all of the samples according to JCPDS Card No. 65–2908 and the present results are also supported by the work of Azzaoui et al. [14]. No peaks associated with Zn, Al, or their composites such as ZnO and Al₂O₃ are evident here which means the samples possess no secondary phases or segregation clarifying the incorporation of Zn and Al into the CdO lattice. Again, the similarity in the profile as obtained following

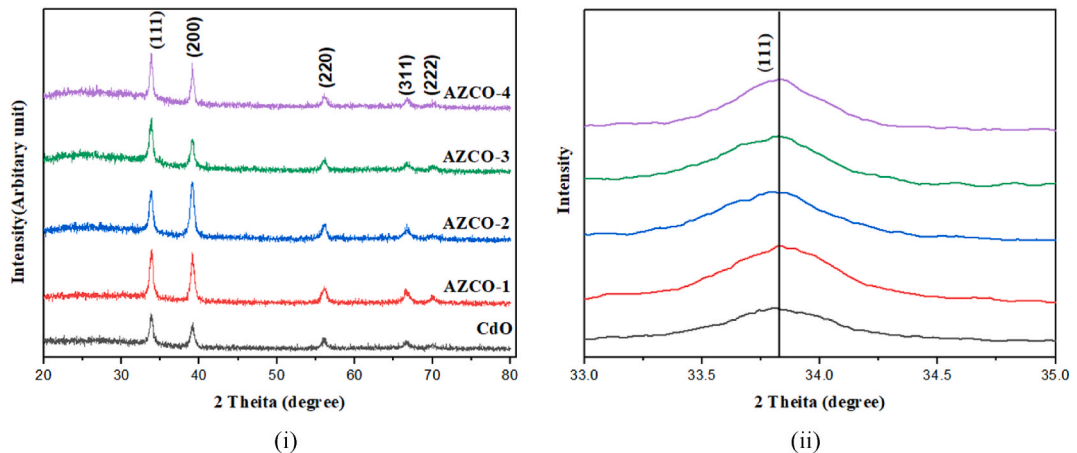


Fig. 2. i) The XRD patterns of CdO, AZCO-1, AZCO-2, AZCO-3 and AZCO-4 and ii) peak shifting of (111) plane.

the (111) plane for pure and zinc-aluminum co-doped samples validates that Cd^{2+} ions are being successfully substituted. However, there an increase in (200) plane intensity was evident. A similar phenomenon was also observed by a few researchers [14]. It is also revealed that the preferential orientation shifted from (111) to (002) directions for 3% (Zn & Al) concentrations which means that more atoms are aligned along this direction in that doping concentration. Afterward, the preferential direction aging changes to (111) directions for higher doping concentrations of Zn. Besides, Fig. 2 (ii) represents the slight peak shifting for (111) due to the ionic radius differences among the Cd^{2+} , Zn^{2+} , and Al^{3+} atoms. From Table 2, it is depicted that there is a slight decrease in the lattice parameter for AZCO-1. This is due to the decrease in interatomic spacing that occurred as a result of co-doping [14]. The phenomenon occurs when smaller ions substitute comparatively larger ions [14].

However, the lattice parameters of un-doped and dual-doped CdO samples are almost similar. This again proves that the dopant atoms have substituted Cd^{2+} ions imparting no change in their crystal structure.

Fig. 3 shows the changes in the structural parameters (obtained from XRD analysis) of deposited thin films with incorporated doping concentration.

The crystallite size of CdO is strongly affected by elemental doping (Table 2). From Tables 2 and it is observed that crystallite first decreases with increasing Zn concentrations and attended a minimum of 10.05 nm for 3% (Zn & Al) concentration and then it shows an increasing trend with increasing doping concentration. A significant decrease in the dislocation density was observed for AZCO-4 while all the samples showed nearly the same value of strain.

3.2. SEM and EDS analysis

The surface morphology of un-doped and dual-doped CdO thin films are depicted in Fig. 4(a–e). In the realm of device technology applications, scanning electron microscopy (SEM) serves as an effective means to assess surface morphology properties [22]. Employing ImageJ software, we determined the average grain diameters to be 228 nm, 207 nm, 164 nm, and 314 nm for doping percentages of Zn ranging from 2%, 3%, 4%, and 5%, respectively. As doping percentages increase, grain size diminishes; however, at 5% doping, a notable increase in grain size was observed. At higher concentrations, particles exhibited improved dispersion, albeit with some interconnection among them. A rough polycrystalline structure with misaligned grains emerged at the 2% doping level, a feature of large grain misalignment crucial for electronic devices involving oxide materials [23].

To investigate the elemental composition of dual-doped CdO films, we utilized energy-dispersive X-ray spectroscopy (EDS). Fig. 5 presents the EDS spectrum for a lower concentration of co-doped film, revealing distinct peaks corresponding to Cd, O, Al, and Zn, thus confirming the presence of co-doped elements. Notably, when employing soda-lime-silicate glass as a substrate, additional peaks attributed to Na and Si were also detected (as shown in Table 3).

3.3. Optical analysis

The transmittance characteristics of both doped and undoped samples are presented in Fig. 6(a), revealing a discernible increase in transmittance values up to 700 wavelengths.

However, beyond this threshold, a reduction in transmittance is evident, except for the 5% concentrated film. Notably, as the doping percentages increase, the transmittance values also exhibit an upward trend. Intriguingly, the 4% concentrated film demonstrates higher transmittance than the 5% counterpart. Several factors contribute to the observed decrease in transmittance. The higher thickness of the 5% concentrated film, as reported in previous studies [15], alongside distortion induced by co-doped ions [12], larger crystallite size [24], and decreased surface roughness [24,25] are identified as potential influencers. It is noteworthy that these factors collectively contribute to the nuanced optical behavior observed in the transmittance spectra.

Fig. 6(b) illustrates a discernible reduction in the extinction coefficient for both doped and undoped samples as the wavelength increases. Moreover, an intriguing trend emerges with increasing doping concentration, indicating a consistent decrease in the extinction coefficient (k). This observation implies that heightened doping percentages contribute to a diminished light-absorbing capacity within the material. Consequently, this phenomenon enhances energy conversion, thereby improving the overall performance of the optoelectronic device. The diminished extinction coefficient and decreased light absorption in the doped materials establish their suitability for efficiently transmitting light through the window layer and into the active regions of the solar cell [26].

Table 2

Obtained structural (XRD) parameters of pure CdO, AZCO-1, AZCO-2, AZCO-3, and AZCO-4 thin films along (111) plane.

Sample	Value of 2 θ at (111)	Crystallite size (nm)	Crystallinity %	Dislocation $\delta \times 10^{-3}$ (lines/m ²)	Strain $\epsilon \times 10^{-3}$	Lattice constant, a (Å)	Volume of unit cell, Å ³	FWHM, $\beta \times 10^{-3}$
CdO	33.83	13.98	42.916	5.109	2.46	4.585	96.386	10.359
AZCO-1	33.69	12.95	61.165	5.960	2.67	4.572	95.569	11.188
AZCO-2	33.79	10.05	56.192	6.671	2.83	4.589	96.386	11.836
AZCO-3	33.78	12.807	53.087	6.096	2.70	4.589	96.639	11.314
AZCO-4	33.81	17.407	46.151	3.300	1.99	4.586	95.569	8.325

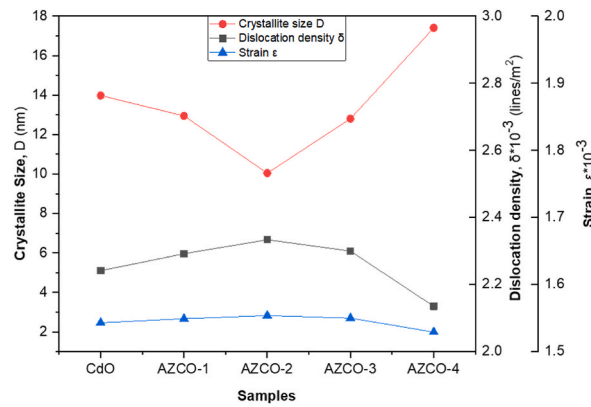


Fig. 3. Variation of crystallite size, dislocation density and strain of the un-doped and (Zn-Al) dual-doped CdO thin films.

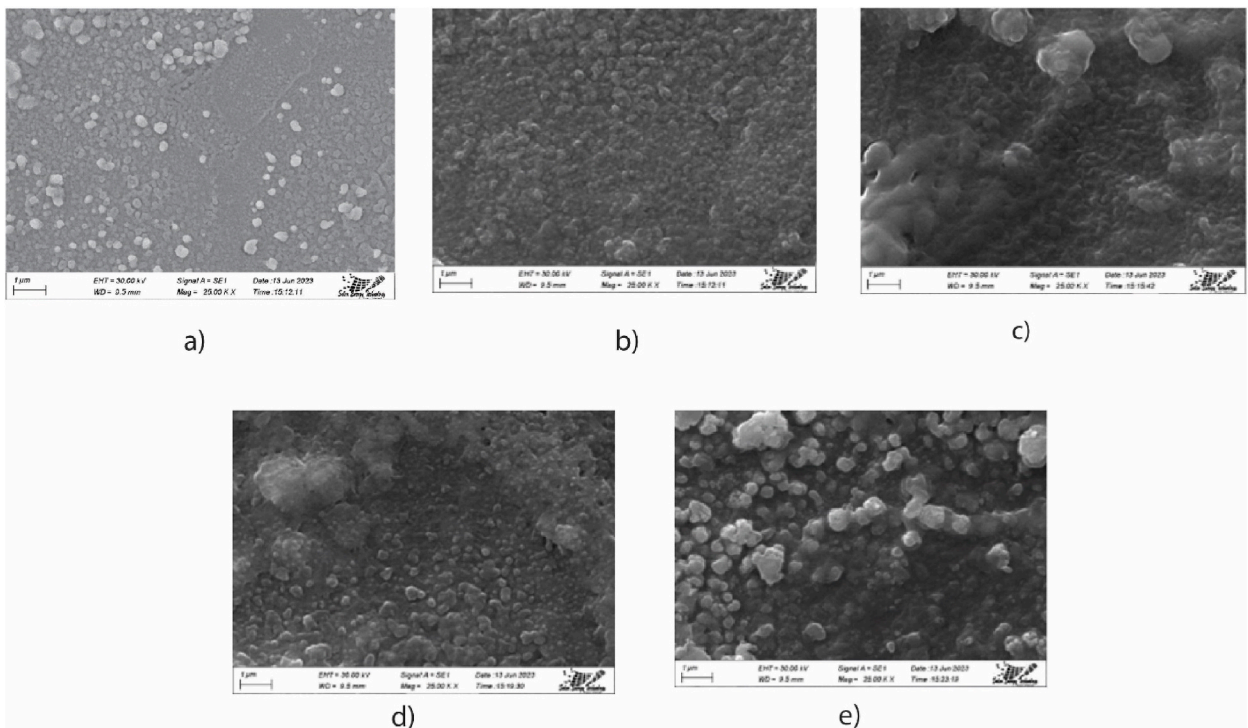


Fig. 4. SEM images of pure (a) CdO, (b) AZCO-1, (c) AZCO-2, (d) AZCO-3, and (e) AZCO-4 thin films.

This crucial optical characteristic underscores the potential of doped thin films to optimize energy conversion processes, positioning them as promising candidates for enhancing the efficiency of solar cell applications.

For direct band gap $n = 2$. The energy band gap of the doped and co-doped films was determined using equation (9), and the values obtained were 2.611, 2.629, 2.64, 3.19, and 3.84 eV, respectively, as shown in Fig. 6(c).

The investigation into the band gap of the thin films reveals a noteworthy increase with escalating doping percentages. This observed trend aligns with expectations, as the introduction of Al^{3+} imparts an additional electron into the lattice, creating an impurity band below the conduction bands. Consequently, the Fermi level penetrates the conduction band, leading to an expansion of the band gap widely recognized as the Moss–Burstein effect.

Corroborating this finding, Zaoui et al. [27] elucidated the impact of Zn doping in CdO, proposing that Zn^{2+} ions replace Cd^{2+} ions in the lattice, resulting in an augmented band gap. The theoretical predictions align seamlessly with our X-ray diffraction (XRD) analysis, particularly noting a rapid increase in band gap values at 4% and 5% Zn concentrations. This suggests the effective substitution of Cd ions within the CdO lattice by Zn and Al ions. Surprisingly, the observed increase in band gap values persists even with higher concentrations of Zinc, indicating a successful incorporation of Zn and Al ions into the CdO lattice. This increase in band gap can be attributed to the concurrent rise in free electron concentration within the films [16]. Although CdO is recognized for its narrow

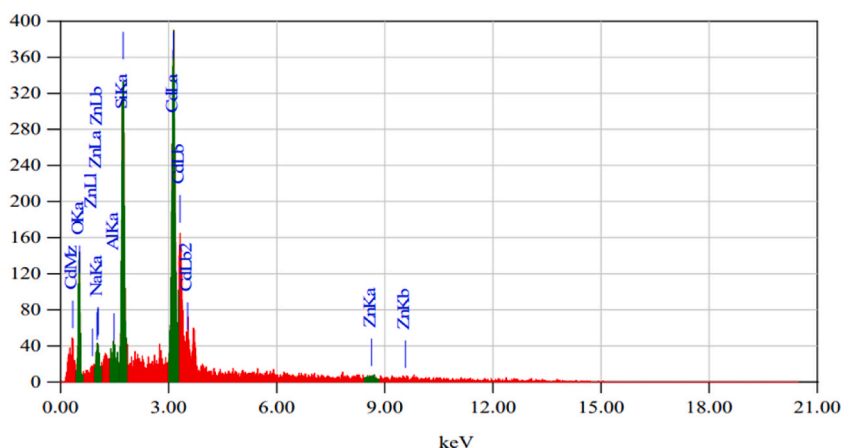


Fig. 5. EDS graph of fabricated AZCO-1 thin film.

Table 3

Elemental information obtained from EDS in terms of mass% and atom% of AZCO-1.

Element	Atom %
O	65.35
Na	1.77
Al	0.99
Si	14.15
Zn	1.13
Cd	16.61

energy band gap [17], the process of doping facilitates the widening of the band gap, rendering it more suitable for diverse applications, notably in solar cells and other optoelectronic devices [17]. Higher band gap values are particularly valuable in military, radio, and power conversion applications as they allow for higher voltages, frequencies, and temperatures to be handled efficiently. The heightened band gap values, particularly notable in the 4% and 5% Zn concentrations, hold significance for applications in military, radio, and power conversion, enabling efficient handling of higher voltages, frequencies, and temperatures. This optical analysis underscores the tailored tunability of CdO thin films through doping, enhancing their suitability for a spectrum of technological applications.

Fig. 6(d) provides insight into the wavelength-dependent refractive index of undoped and co-doped CdO thin films. Notably, as the wavelength extends, the refractive index values exhibit an initial increase, reaching a critical point where a subsequent decline occurs. Up to a wavelength of 600, the refractive index of CdO films demonstrates a consistent rise with increasing Zn doping concentration. This trend is attributed to the heightened surface roughness of the films, a conclusion supported by the SEM.

However, beyond the 600-wavelength point, a convergence is observed among all concentrated films, resulting in similar refractive index values. This aligns with findings reported by W. Azzaoui et al. [14] in a study encompassing both undoped and 3% co-doped CdO films within the same wavelength region. In parallel, Fig. 6(e) illustrates that an increase in doping concentration correlates with a decrease in the absorption coefficient as the wavelength increases. This intricate relationship underscores the interplay between doping concentration and optical properties, offering valuable insights into the nuanced behavior of CdO thin films in different spectral regions. The observed trends in refractive index and absorption coefficient contribute to a comprehensive understanding of the optical characteristics of co-doped CdO thin films, providing a foundation for their potential applications in optoelectronic devices and other relevant technologies.

Fig. 6(e) illustrates the variation of the absorption coefficient with wavelength. A discernible decreasing trend in the absorption coefficient is observed with an increase in doping concentration. Simultaneously, a consistent decline in reflectance is noted after reaching a short-lived maximum. The observed alterations in reflectance align with corresponding changes in the film's characteristics, emphasizing a clear correlation. The diminishing absorption coefficient and reflectance patterns are indicative of the tailored optical behavior achieved through the modulation of doping concentration. This nuanced control over optical properties holds significance, particularly for applications requiring films with low reflectivity and higher transmittance values. Such characteristics are notably advantageous for window layer applications, as emphasized in previous studies [15].

3.4. Electrical analysis

Fig. 7 illustrates the variation in resistivity with doping concentration. These results have been compared in Table 4 with data

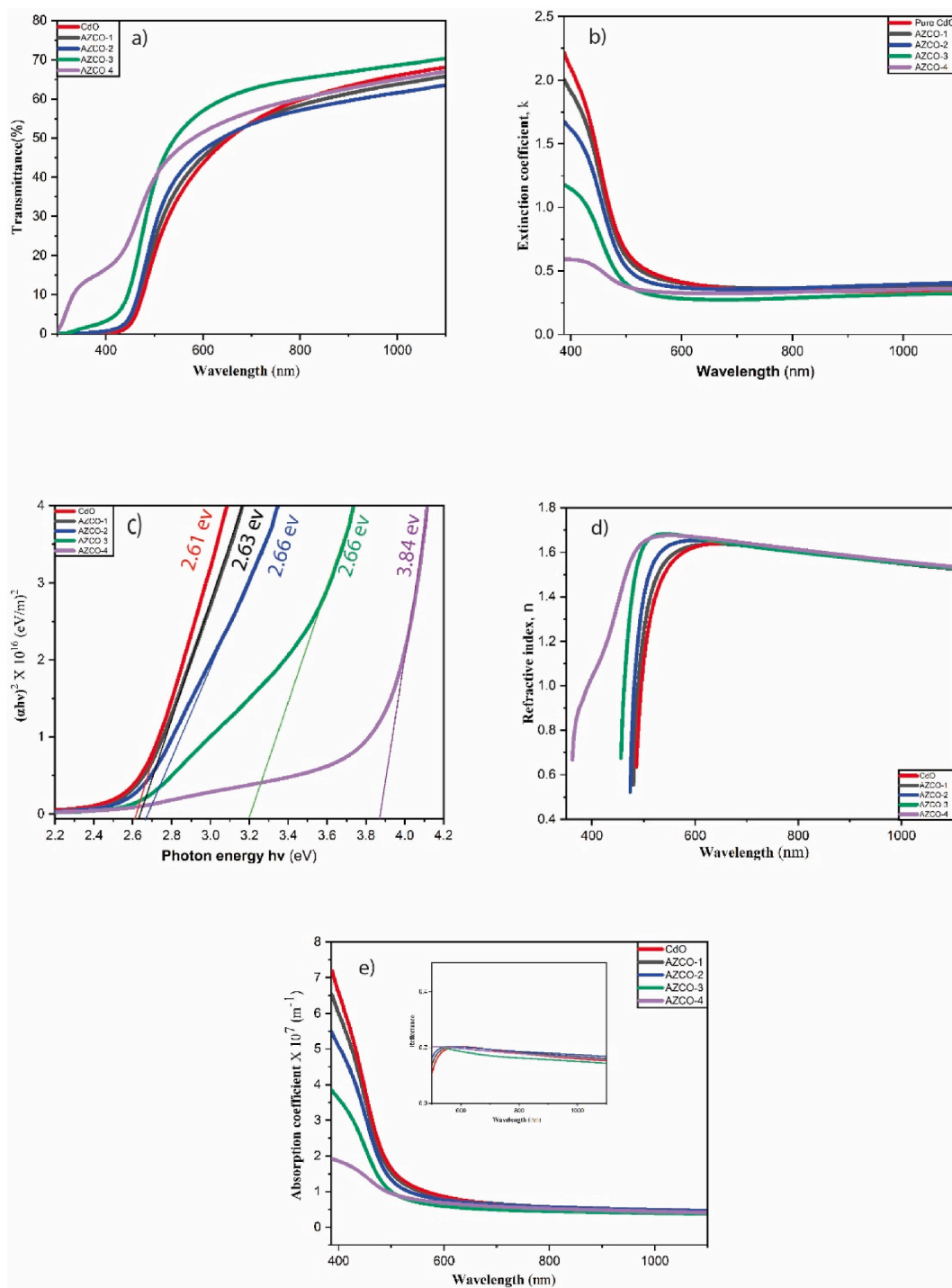


Fig. 6. Variation of (a) optical transmittance, (b) extinction coefficient, (c) optical band gap with photon energy, (d) refractive index, and (e) absorption coefficient of deposited thin films.

reported in previous studies employing different techniques and dopants.

The resistivity of the films exhibited a decreasing trend as the Zn doping concentration increased up to 3%. However, beyond this point, with further increases in Zn concentration, the resistivity began to rise. Notably, the highest conductivity was observed at a 2% Zn concentration, which was attributed to the enhanced crystallinity identified through XRD analysis. This improved crystallinity played a pivotal role in reducing resistivity.

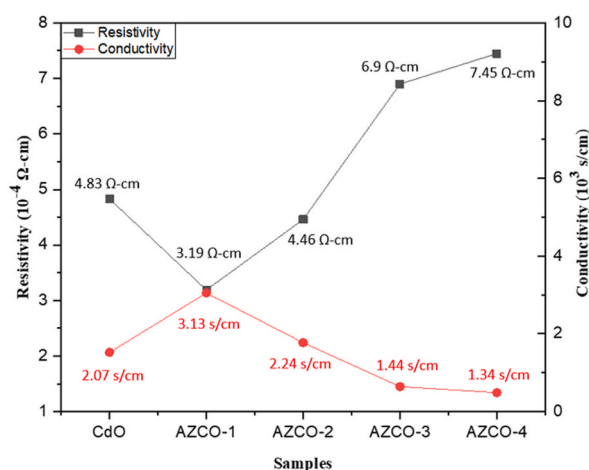


Fig. 7. Comparison of resistivity and conductivity of pure CdO, AZCO-1, AZCO-2, AZCO-3 and AZCO-4 films.

Table 4

Comparative analysis between (Zn–Al) dual-doped CdO thin films and previously published works.

Sample	Transparency (%) (600–800 nm)	Calculated or experimentally obtained conductivity, S/cm	Method	Reference
CdO (0 wt %)	44–59	2.07×10^3	Spray Pyrolysis	Present Work
CdO (4% Zn 3% Al)	57–65	1.44×10^3	Spray Pyrolysis	Present Work
CdO (3% Zn 1% Al)	50–68	7.57×10^3	Spray Pyrolysis	[14]
CdO (4% Sr)	30–49	1.30×10^3	Spray Pyrolysis	[21]
CdO (2.5 wt%Zn,4 wt% Co)	79–80	0.077×10^3	Spray Pyrolysis	[12]
CdO (2.5 wt%Zn,2 wt% Co)	80–82	0.054×10^3	Spray Pyrolysis	[12]
CdO: Al (5 at. %)	63–82	0.370×10^3	RF sputtering	[7]
CdO: Al (2 at. %)	69 at 30 °C	35.571×10^3	Pulsed Laser Deposition	[28]

Subsequently, as the Zn concentration was increased from 2% to 5%, crystallinity decreased, leading to an increase in the number of defects within the thin films. This increase in defects resulted in higher resistivity compared to pure CdO. It was observed that Zn^{2+} ions, occupying interstitial positions, acted as traps for free carriers, contributing to the observed increase in resistivity [29].

4. Conclusion

In this study, Zn–Al dual-doped cadmium oxide (AZCO) and undoped cadmium oxide (CdO) thin films were successfully deposited on glass substrates using the spray pyrolysis method at a deposition temperature of 325 °C. Our investigation revealed that the concentration of Zn doping significantly influences the morphological, optical, electrical, and structural characteristics of the CdO thin films. X-ray Diffraction (XRD) analysis confirmed the films' cubic shape with a polycrystalline nature, where a noticeable change in the (100) peak and EDS results verified the successful doping of our samples. SEM analysis highlighted morphological changes, presenting rock-like structures with dual-doping concentrations of Zn and Al. The optical properties of the films were characterized using UV–visible spectroscopy, while the four-probe method was employed to determine the electrical resistivity. Our results demonstrated that AZCO-1 exhibited the highest percentage of crystallinity and electrical conductivity. Conversely, AZCO-5 exhibited the highest crystallite size and band gap. This research underscores the profound impact of varying concentrations of Zn and Al on the properties of CdO deposited on glass substrates. The versatility of these films positions them for applications in optoelectronics and thermal barrier coatings. The successful manipulation of the film properties, especially in terms of crystallinity, electrical conductivity, and band gap, opens avenues for tailoring these materials to specific technological requirements. Overall, our findings contribute valuable insights to the design and utilization of Zn–Al dual-doped CdO thin films for diverse applications in materials science and technology.

Funding

The contributors received no funding and all the costs associated with this research are self-funded.

Data availability statement

Data will be made available on request.

CRedit authorship contribution statement

M Ashikul Haque Naeem: Writing – original draft, Software, Funding acquisition, Formal analysis, Data curation, Conceptualization. **Ahmed Sidrat Rahman Ayon:** Writing – original draft, Software, Methodology, Investigation, Funding acquisition, Formal analysis. **Md. Mintu Ali:** Writing – review & editing, Supervision, Project administration, Formal analysis, Conceptualization. **Md. Ruhul Amin:** Visualization, Validation, Methodology. **M. Humayan Kabir:** Writing – review & editing, Visualization, Validation, Resources. **Md. Abdus Sattar:** Writing – review & editing, Visualization, Project administration, Formal analysis. **Samia Tabassum:** Visualization, Validation, Investigation, Data curation. **Md Nurul Huda Liton:** Writing – review & editing, Visualization, Validation, Investigation.

Declaration of competing interest

The authors declare that they have no known competing financial interests or personal relationships that could have appeared to influence the work reported in this paper.

Acknowledgments

The authors are grateful to the Glass & Ceramic Engineering (GCE) department of Rajshahi University of Engineering & Technology (RUET), Department of Material Science & Engineering (MSE) and Department of Physics, University of Rajshahi (RU), and Bangladesh Council of Scientific and Industrial Research (BCSIR), Dhaka, for the providing the scope to conduct the research and its associated testing facilities.

References

- [1] T. Minami, Transparent conductive oxides for transparent electrode applications, *semicond, Semimetals* 88 (2013) 159–200, <https://doi.org/10.1016/B978-0-12-396489-2.00005-9>.
- [2] K.L. Chopra, S. Major, D.K. Pandya, *Review Paper* 102 (1983) 1–46.
- [3] X. Wu, W.P. Mulligan, T.J. Courts, *Developments in RF Sputtered Cadmium Starmate Films*, vol. 286, 1996, pp. 274–276.
- [4] A. Abdulhameed, M. Mahadi, H. Wan, M. Wan, A. Kamil, K. Ooi, Influence of carbon nanotube suspensions on the structural, optical, and electrical properties of grown ZnO nanorods, *Appl. Phys. A* (2023), <https://doi.org/10.1007/s00339-023-06801-z>.
- [5] Y.S.M. Elzawiei, A. Abdulhameed, R. Hashim, M.M. Halim, A study of the UV photodetectors properties based on the effect of TiO₂ on ZnO nanorods grown via the chemical bath deposition method on p-type Si (100) substrates, *Opt. Mater.* 144 (2023) 114353, <https://doi.org/10.1016/j.optmat.2023.114353>.
- [6] A. Abdulhameed, Y. Mahnashi, Fabrication of carbon nanotube/titanium dioxide nanomaterials-based hydrogen sensor using novel two-stage dielectrophoresis process, *Mater. Sci. Semicond.* 167 (2023) 107794, <https://doi.org/10.1016/j.mssp.2023.107794>.
- [7] B. Saha, S. Das, K.K.A. Chattopadhyay, Electrical and Optical Properties of Al Doped Cadmium Oxide Thin Films Deposited by Radio Frequency Magnetron Sputtering, vol. 91, 2007, pp. 1692–1697, <https://doi.org/10.1016/j.solmat.2007.05.025>.
- [8] A.A. Dakhel, *Generation of Magnetic Properties in Degenerated Ni and Ga Codoped CdO Nanocrystals*, 2020.
- [9] M.B.A.A. Dakhel, M. El-Hilo, Ferromagnetic Properties of Cu- and Fe-Codoped Nanocrystalline CdO Powders: Annealing in Hydrogen Promote Long-Range Ferromagnetic Order, vol. 6, 2014, <https://doi.org/10.1016/j.appt.2014.07.015>.
- [10] A.A. Dakhel, O-4, Optoelectronic Properties of Eu- and H-Codoped CdO Films, vol. 11, 2011, <https://doi.org/10.1016/j.cap.2010.06.003>.
- [11] C. Bhukkal, R. Ahlawat, Cu²⁺–Mn²⁺–Co-doped CdO nanocrystallites: comprehensive research on phase, morphology and optoelectronic properties, *Res. Chem. Intermed.* (2020), <https://doi.org/10.1007/s11164-020-04202-y>.
- [12] T. Noorunnisha, M.S.M. Karthika, C.K.K. Usharani, S. Balamurugan, (Zn + Co) co - doped CdO thin films with improved figure of merit values and ferromagnetic orderings with low squareness ratio well suited for optoelectronic devices and soft magnetic materials applications, *Appl. Phys. A* (2020) 1–9, <https://doi.org/10.1007/s00339-020-03954-z>.
- [13] M. Banuprakash, B. Abhishek, H. Acharya, R. Bairy, S. Bhat, H. Vijeth, M.S. Murari, A. Jayarama, R. Pinto, Materials Today : proceedings Structural, linear and nonlinear optical characterization of Ni and Al Co-Doped CdO semiconductor nanostructures for nonlinear optical device applications, *Mater. Today Proc.* (2020), <https://doi.org/10.1016/j.matpr.2020.02.766>.
- [14] W. Azaoui, M. Medles, R. Miloua, A. Nakrela, A. Bouzidi, M. Khadraoui, F. Bessuelle, R. Desfeux, Rietveld refinement combined with first-principles study of Zn and Al – Zn doped CdO thin films and their structural, optical and electrical characterisations 1010 (2023), <https://doi.org/10.1007/s10854-023-10384-z>.
- [15] M.K.R. Khan, M.A. Rahman, M. Shahjahan, M.M. Rahman, M.A. Hakim, D. Kumar, J. Uddin, Effect of Al-doping on optical and electrical properties of spray pyrolytic nano-crystalline CdO thin films, *Curr. Appl. Phys.* 10 (2010) 790–796, <https://doi.org/10.1016/j.cap.2009.09.016>.
- [16] R. Kumaravel, S. Menaka, S.R. Mary, K. Ramamurthi, K. Jeganathan, Electrical, optical and structural properties of aluminum doped cadmium oxide thin films prepared by spray pyrolysis technique, *Mater. Chem. Phys.* 122 (2010) 444–448, <https://doi.org/10.1016/j.matchemphys.2010.03.022>.
- [17] K.U.A.R. Balu, Structural, Optical, and Electrical Properties of Zn-Doped CdO Thin Films Fabricated by a Simplified Spray Pyrolysis Technique, 2014, <https://doi.org/10.1007/s40195-014-0168-6>.
- [18] V. Uvarov, I. Popov, ScienceDirect Metrological characterization of X-ray diffraction methods at different acquisition geometries for determination of crystallite size in nano-scale materials, *Mater. Char.* 85 (2013) 111–123, <https://doi.org/10.1016/j.matchar.2013.09.002>.
- [19] N. Manjula, A.R. Balu, Double doping (Mn+Cl) effects on the structural, morphological, photoluminescence, optoelectronic properties and antibacterial activity of CdO thin films, *Opt. - Int. J. Light Electron Opt.* (2016), <https://doi.org/10.1016/j.jileo.2016.10.074>.
- [20] R. Kumaravel, K. Ramamurthi, V. Krishnakumar, Journal of Physics and Chemistry of Solids Effect of indium doping in CdO thin films prepared by spray pyrolysis technique, *J. Phys. Chem. Solid.* 71 (2010) 1545–1549, <https://doi.org/10.1016/j.jpcs.2010.07.021>.
- [21] M.H. Kabir, A. Bhattacharjee, M.M. Islam, M.S. Rahman, Effect of Sr doping on structural, morphological, optical and electrical properties of spray pyrolyzed CdO thin films, *J. Mater. Sci. Mater. Electron.* 32 (2021) 3834–3842, <https://doi.org/10.1007/s10854-020-05127-3>.
- [22] M. Yüksel, B. Ş. F. Bayansal, Nano Structured CdO Films Grown by the SILAR Method : in Fl Uence of Silver-Doping on the Morphological, Structural and Optical Properties, 2016, <https://doi.org/10.1016/j.ceramint.2015.12.154>.
- [23] N. Cristì, S. Vieira, E. Giuliani, R. Fernandes, A. Antonio, A. De Queiroz, Indium tin oxide synthesized by a low cost route as SEGFT pH, *Sensor* 16 (2013) 1156–1160, <https://doi.org/10.1590/S1516-14392013005000101>.
- [24] S. Ahmed, M.S.I. Sarkar, M.M. Rahman, M. Kamruzzaman, M.K.R. Khan, E Ff Ect of Yttrium (Y) on Structural, Morphological and Transport Properties of CdO Thin Films Prepared by Spray Pyrolysis Technique, *Heliyon*, 2018 e00740, <https://doi.org/10.1016/j.heliyon.2018.e00740>.
- [25] M. Ashaduzzman, M.K.R. Khan, A.M.M.T. Karim, M.M. Rahman, Influence of Chromium on structural, non-linear optical constants and transport properties of CdO thin films, *Surface. Interfac.* (2018), <https://doi.org/10.1016/j.surfin.2018.05.008>.

- [26] D.M.A. Latif, I.H. Shallal, A.A. Shuihab, H. Shallal, A. Shuihab, ScienceDirect ScienceDirect ScienceDirect ScienceDirect Synthesis and study of some physical properties of cadmium the and 15th study Synthesis of some physical properties of cadmium oxide CdO thin films oxide CdO thin films Assessing the feasibility of using the heat demand-outdoor Aliyah heat temperature function district demand forecast, Energy Proc. 157 (2019) 611–618, <https://doi.org/10.1016/j.egypro.2018.11.226>.
- [27] A. Zaoui, M. Zaoui, S. Kacimi, A. Boukortt, B. Bouhafs, Stability and Electronic Properties of Zn X Cd 1 – X O Alloys, vol. 120, 2010, pp. 98–103, <https://doi.org/10.1016/j.matchemphys.2009.10.027>.
- [28] R.K. Gupta, K. Ghosh, R. Patel, S.R. Mishra, P.K. Kahol, Preparation and characterization of highly conducting and transparent Al doped CdO thin films by pulsed laser deposition, Curr. Appl. Phys. 9 (2009) 673–677, <https://doi.org/10.1016/j.cap.2008.06.004>.
- [29] N. Manjula, A.R. Balu, K. Usharani, N. Raja, V.S. Nagarethinam, Enhancement in some physical properties of spray deposited CdO:Mn thin films through Zn doping towards optoelectronic applications, Opt. - Int. J. Light Electron Opt. (2016), <https://doi.org/10.1016/j.ijleo.2016.04.129>.